atmosphere

MDPI

Supplementary Material

Trend Analysis and Spatial Source Attribution of Surface Ozone in Chaozhou, China

Zhongwen Huang[1,*], Lei Tong[2,3,*], Xuchu Zhu[4], Junxiao Su[2, 3, 5], Shaoyun Lu[6], Hang Xiao[2, 3]

[1] School of Chemistry and Environmental Engineering, Hanshan Normal University, Chaozhou 521041, China
[2] Center for Excellence in Regional Atmospheric Environment & Fujian Key Laboratory of Atmospheric Ozone Pollution Prevention & Key Laboratory of Urban Environment and Health, Institute of Urban Environment, Chinese Academy of Sciences, Xiamen 361021, China; jxsu@iue.ac.cn (J.S.); hxiao@iue.ac.cn (H.X.)
[3] Zhejiang Key Laboratory of Urban Environmental Process and Pollution Control, CAS Haixi Industrial Technology Innovation Center in Beilun, Ningbo 315830, China
[4] Environmental Protection Monitoring Station in Beilun, Ningbo 315800, China; xuchu_zhu@163.com
[5] University of Chinese Academy of Sciences, Beijing 100049, China
[6] Centre for Chaozhou Environment Information, Chaozhou 521000, China; lushaoyun006@126.com
* Correspondence: huangzw@hstc.edu.cn (Z.H.); ltong@iue.ac.cn (L.T.)

Abbreviations Index

air quality index (AQI)
analysis of variance (ANOVA)
daily maximum 8-hour moving average ozone (MDA8 O_3)
hybrid single-particle Lagrangian integrated trajectory (HYSPLIT)
Kolmogorov-Zurbenko (KZ)
potential source contribution function (PSCF)
Pearl River Delta (PRD)
trajectory sector analysis (TSA)

Caption for All the Figures/Tables

Figure S1. Monthly meteorological data of Chaozhou city in 2023.
Figure S2. The backward trajectory during the first 6 h at study site.
Figure S3. A linear regression analysis of the annual maximum values of MDA8 O_3.
Figure S4. Backward trajectories for different clusters at the study site from 1 January 2020 to 31 December 2023.
Figure S5. Seasonal distribution map of PSCF values for MAD8 O_3.
Figure S6. A quantile-quantile (Q-Q) plot of $W(t)$.
Figure S7. Quantile regression coefficient of O_3 ((**a**) coefficient of independent variable x; (**b**) Constant C).
Figure S8. Backward trajectories at study site for each season, from 1 January 2020 to 31 December 2023.
Figure S9. NWVOC (**a**) and NOx (**b**) emissions in the area surrounding the study site in 2020 (Data source: MEIC emission data for China, http://meicmodel.org.cn).

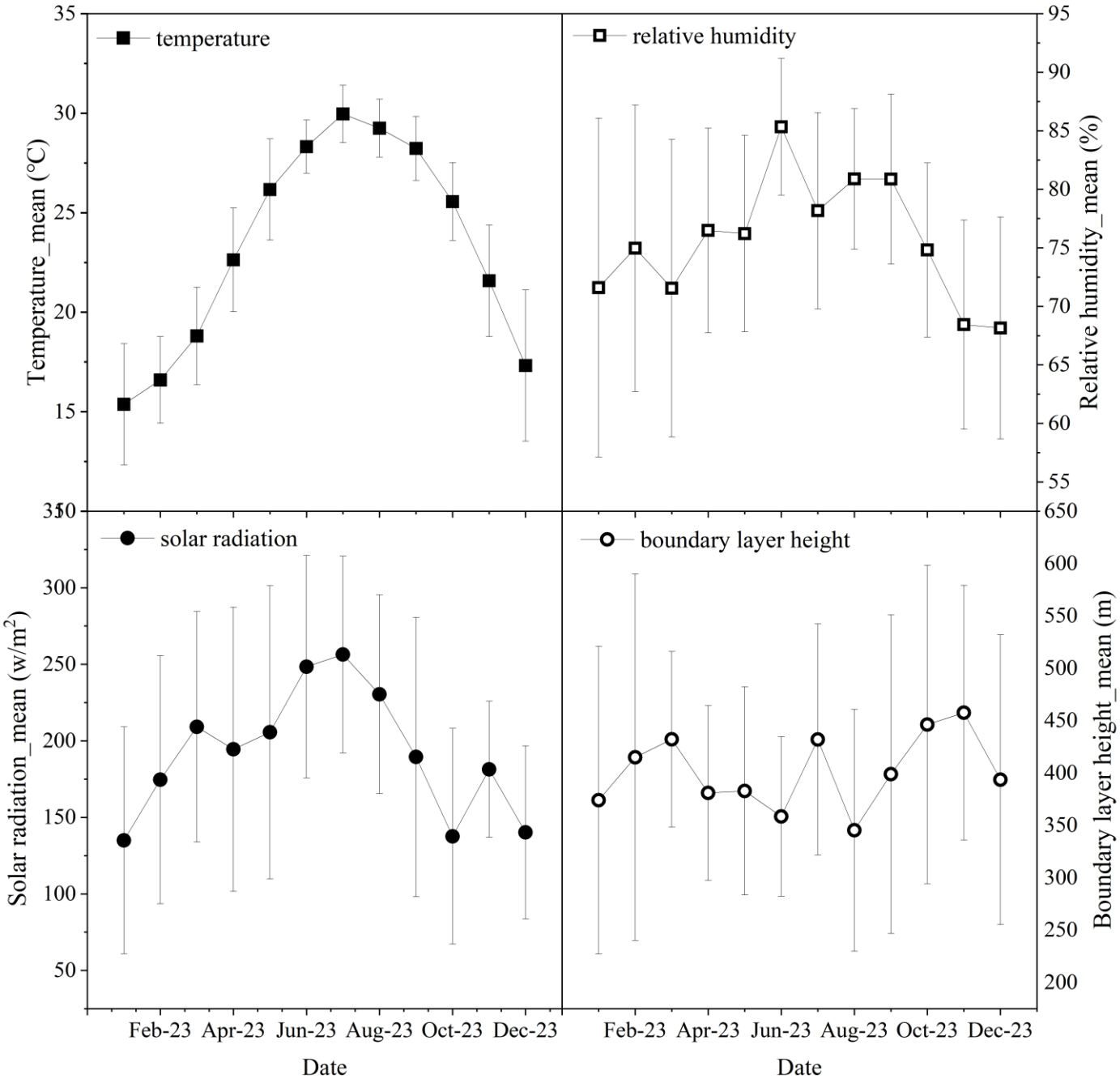

Figure S1. Monthly meteorological data of Chaozhou city in 2023.

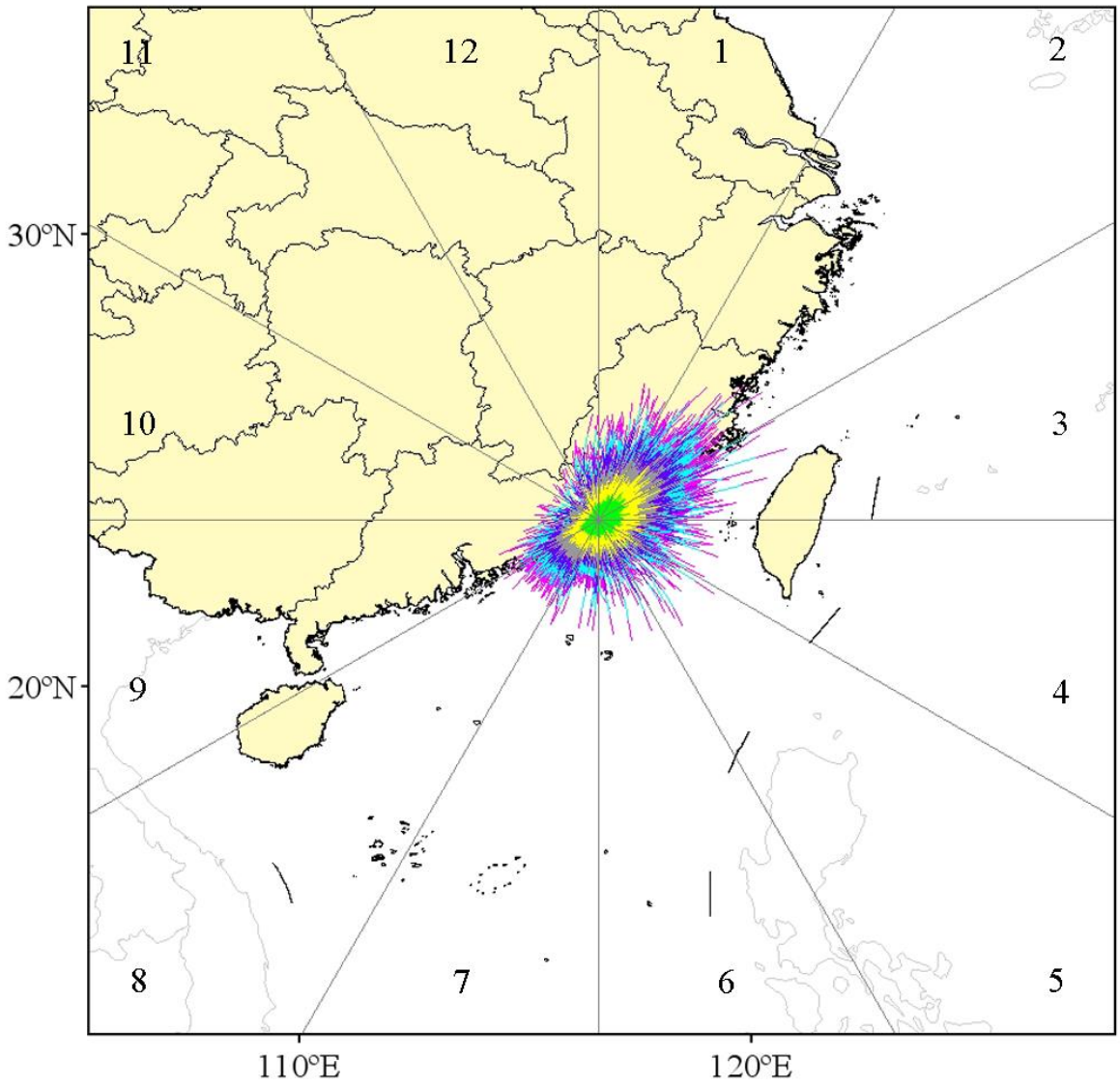

Figure S2. The backward trajectory during the first 6 h at study site.

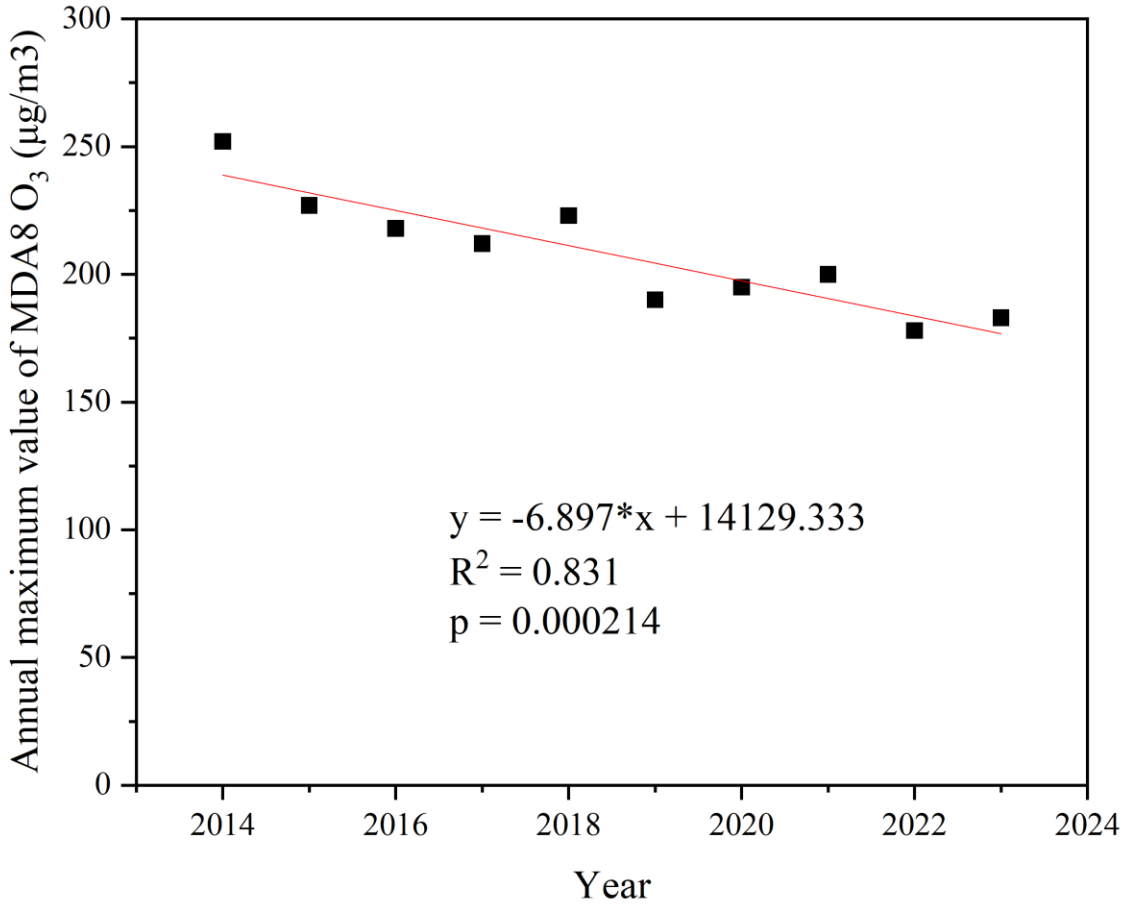

Figure S3. A linear regression analysis of the annual maximum values of MDA8 O_3.

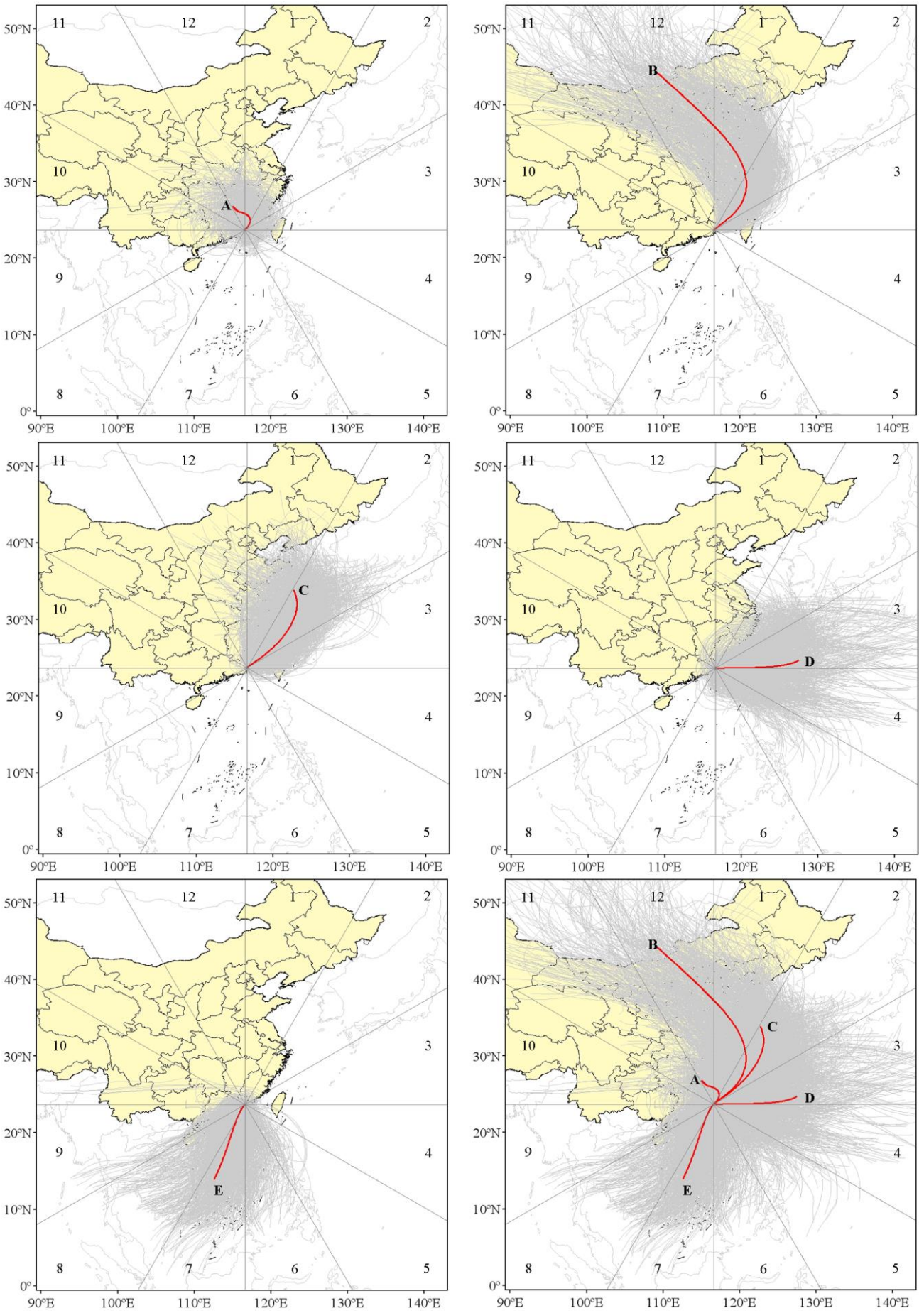

Figure S4. Backward trajectories for different clusters at the study site from 1 January 2020 to 31 December 2023.

57

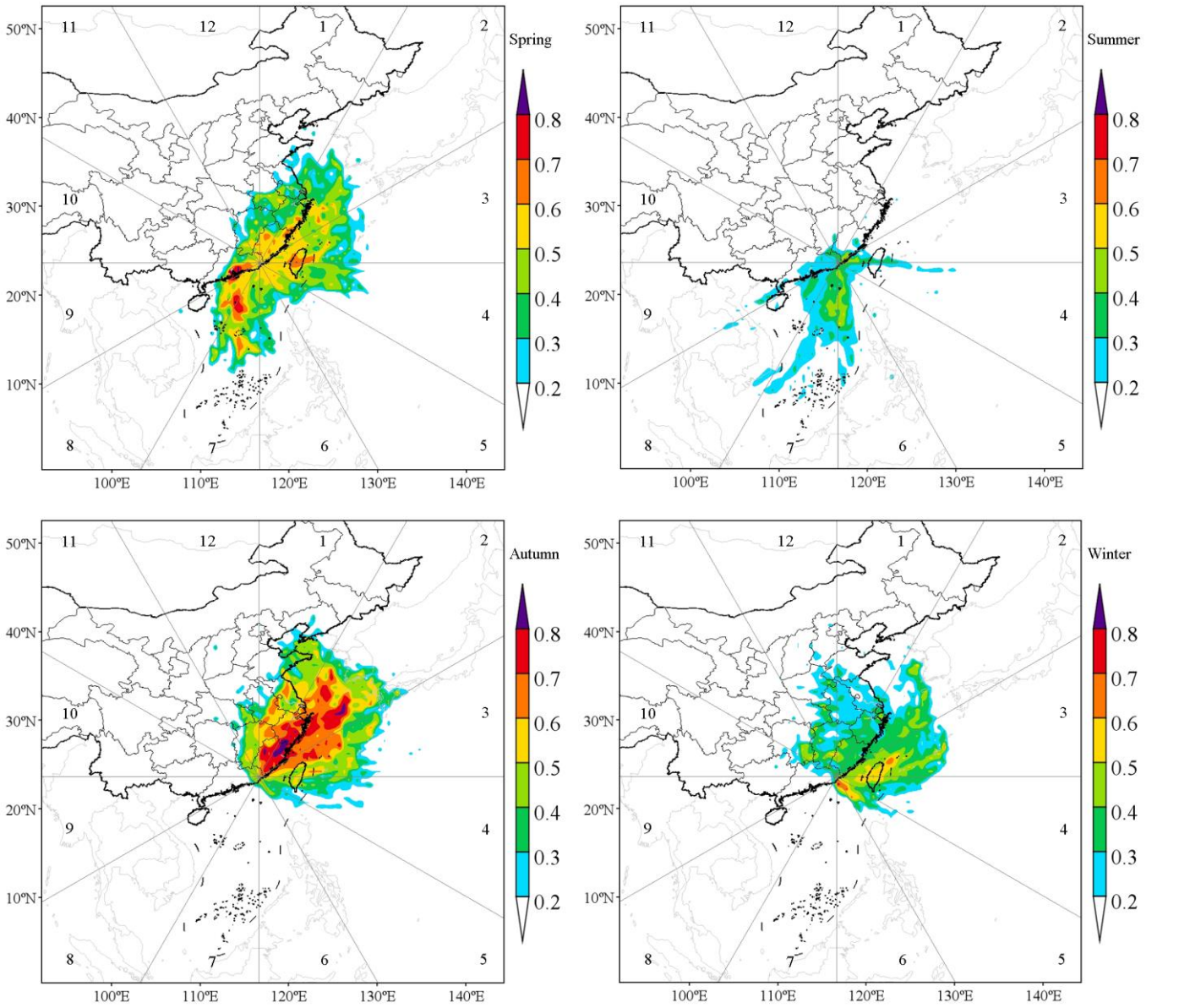

Figure S5. Seasonal distribution map of PSCF values for MAD8 O_3.

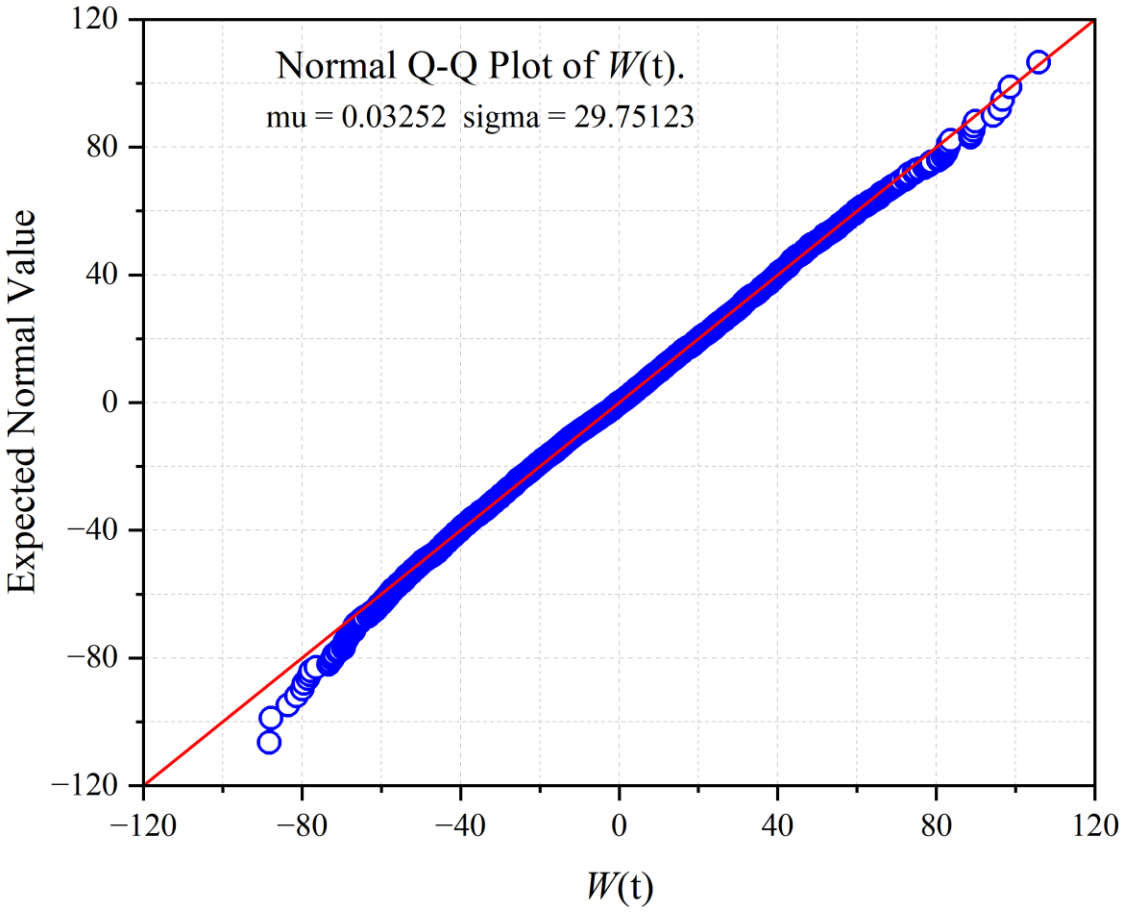

Figure S6. A quantile-quantile (Q-Q) plot of *W*(t).

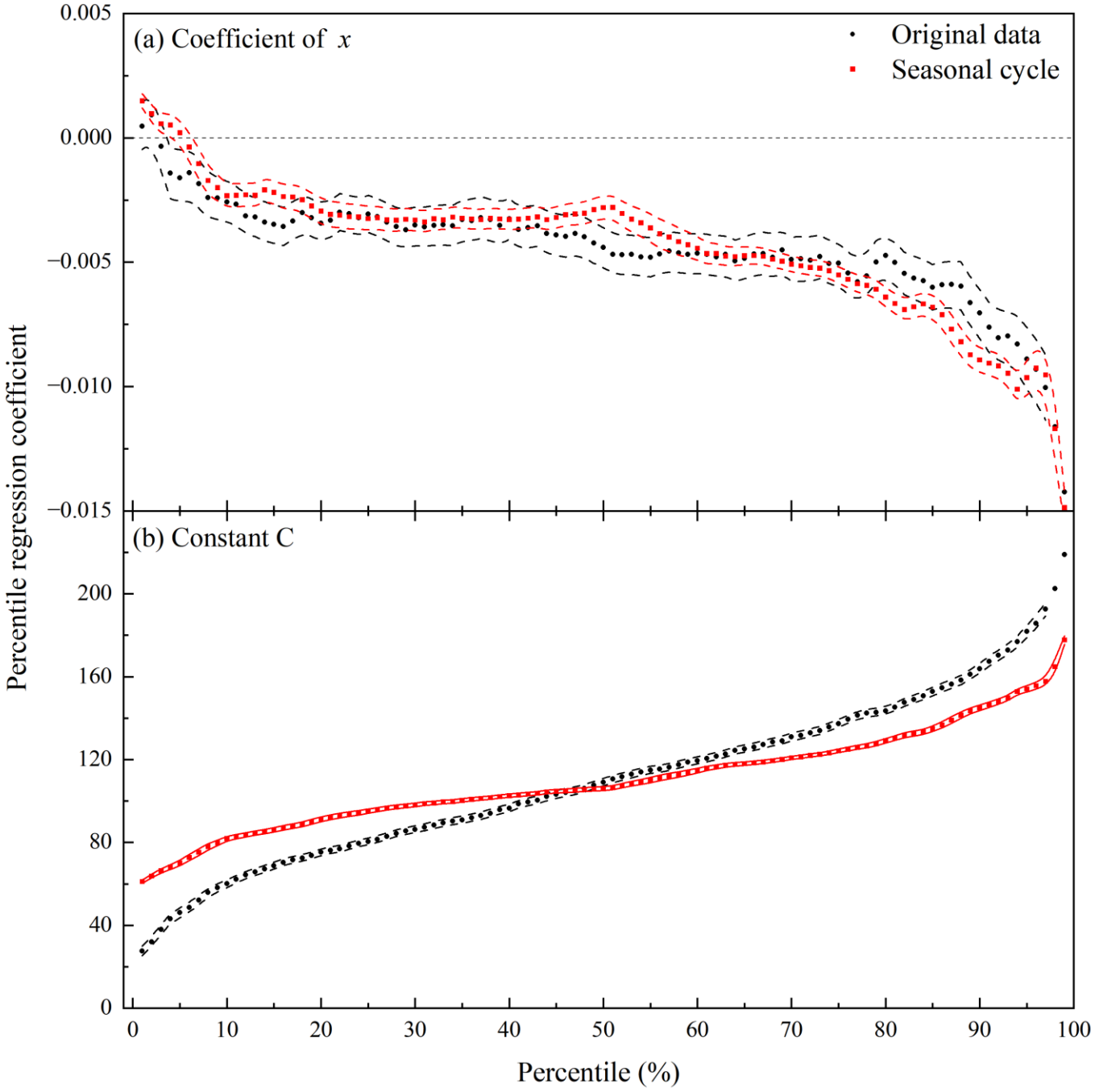

Figure S7. Percentile regression coefficient of O_3 ((**a**) coefficient of independent variable x; (**b**) Constant C).

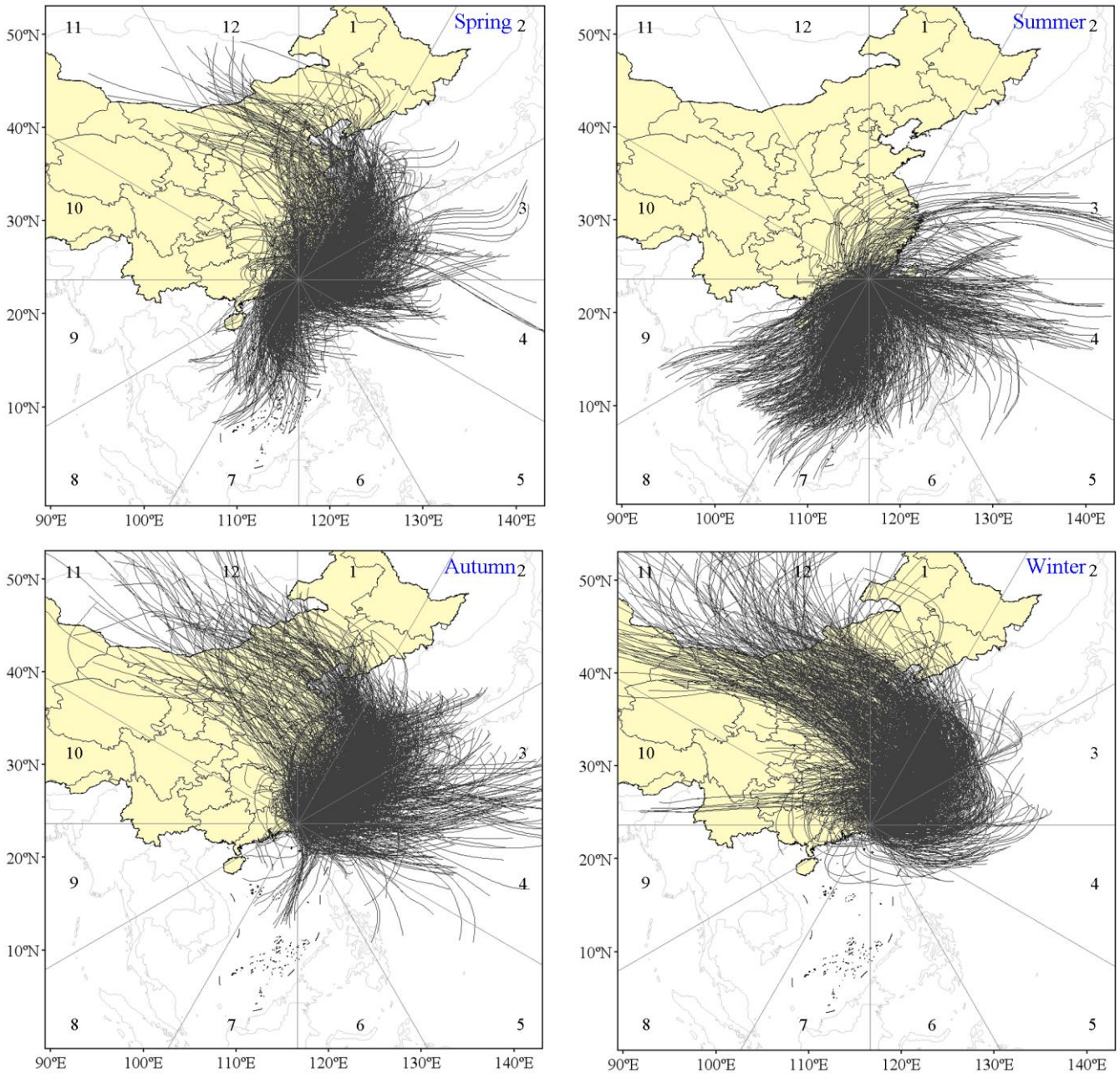

Figure S8. Backward trajectories at study site for each season, from 1 January 2020 to 31 December 2023.

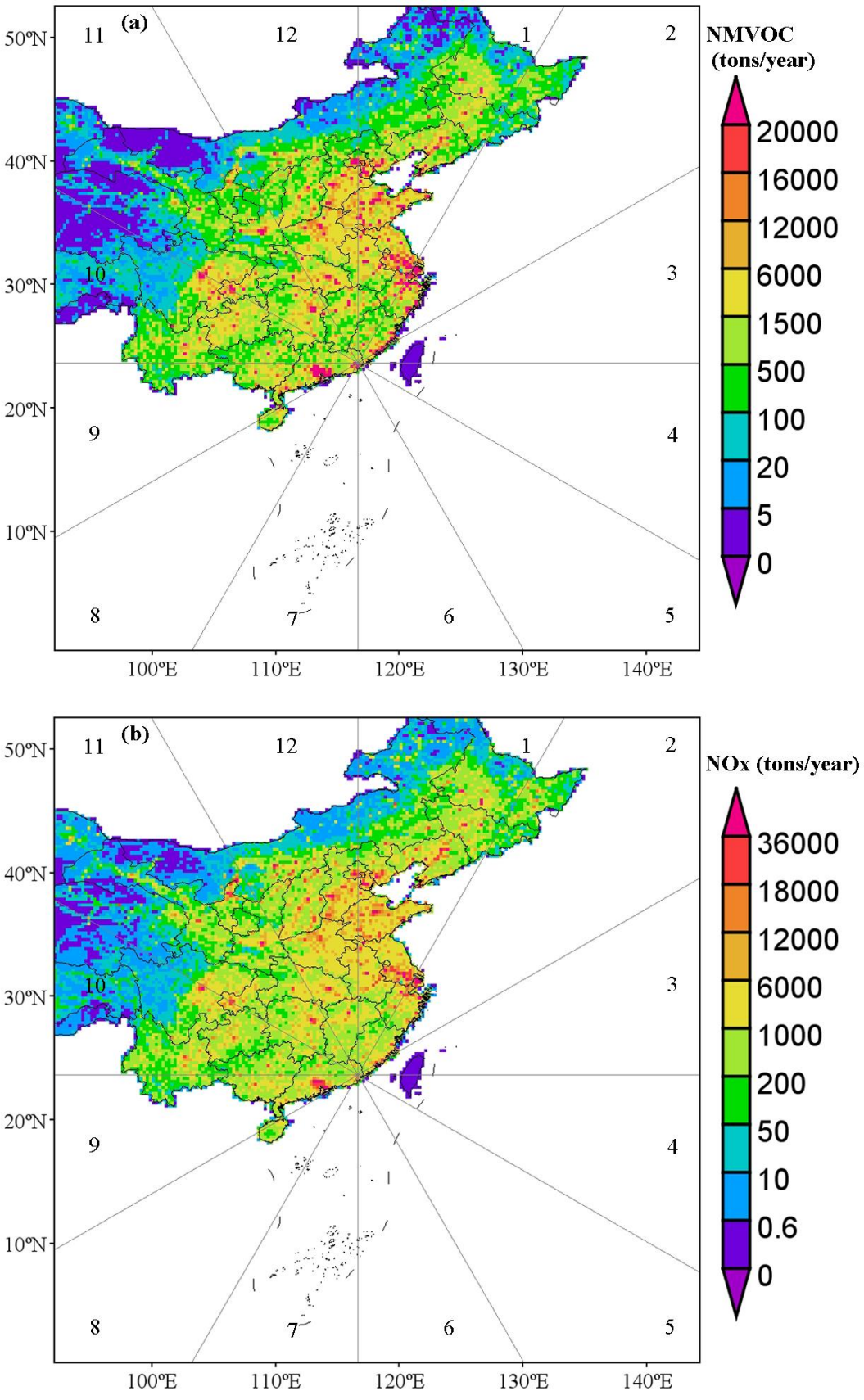

Figure S9. NWVOC (**a**) and NOx (**b**) emissions in the area surrounding the study site in 2020 (Data source: MEIC emission data for China, http://meicmodel.org.cn).